Supplementary Information to

Biospeciation of various antidiabetic $V^{IV}O$ compounds with serum proteins†

Tamás Jakusch,[1] Dominik Hollender,[1] Éva Anna Enyedy,[1] Cristina Sánchez González,[2] Maria Montes-Bayón,[2] Alfredo Sanz-Medel,*[2] João Costa Pessoa,[3] Isabel Tomaz[3] and Tamás Kiss*[1]

---

[1] *Department of Inorganic and Analytical Chemistry, University of Szeged, P.O. Box 440, Szeged H-6701, Hungary, Tel.: +36-62-544337, Fax: +36-62-420505), E-mail: tkiss@chem.u-szeged.hu*

[2] *Department of Physical and Analytical Chemistry. University of Oviedo. C/Julián Clavería 8, 33006 Oviedo, Spain, Tel.: +34-98-5103474, Fax: +34-98-5103474, E-mail: asm@uniovi.es*

[3] *Centro Química Estrutural, Instituto Superior Técnico, TU Lisbon, Av. Rovisco Pais, 1049-001 Lisboa, Portugal*

† Electronic Supplementary Information (ESI) available: CD spectral parameters and CD and EPR spectra.

Table S1 CD spectral parameters of the binary and ternary $V^{IV}O$-apoTf complexes, ($(V^{IV}O)_x$apoTf$(A)_y$. x=1-2, y=0-2; A ≡ dhp or mal, pH 7.4, c(HCO_3^-) = 25.0 mM, T = 25 °C).

	$\lambda_{min}/\Delta\,\varepsilon_{min}$	$\lambda_{max}/\Delta\,\varepsilon_{max}$
	[nm]/[$M^{-1}cm^{-1}$]	
($V^{IV}O$)apoTf	621 / -0.204	754 / 0.053
	918 / -0.290	
$(V^{IV}O)_2$apoTf	621 / -0.408	754 / 0.106
	918 / -0.580	

A	dhp		mal	
	$\lambda_{min}/\Delta\,\varepsilon_{min}$	$\lambda_{max}/\Delta\,\varepsilon_{max}$	$\lambda_{min}/\Delta\,\varepsilon_{min}$	$\lambda_{max}/\Delta\,\varepsilon_{max}$
	[nm]/[$M^{-1}cm^{-1}$]			
($V^{IV}O$)apoTf(A)	635 / -0.360		645 / -0.496	
$(V^{IV}O)_2$apoTf(A)	Not measured		636 / -0.994	812 / 0.242
			876 / -0.190	
$(V^{IV}O)_2$apoTf$(A)_2$	633 / -0.669		639 / -0.993	

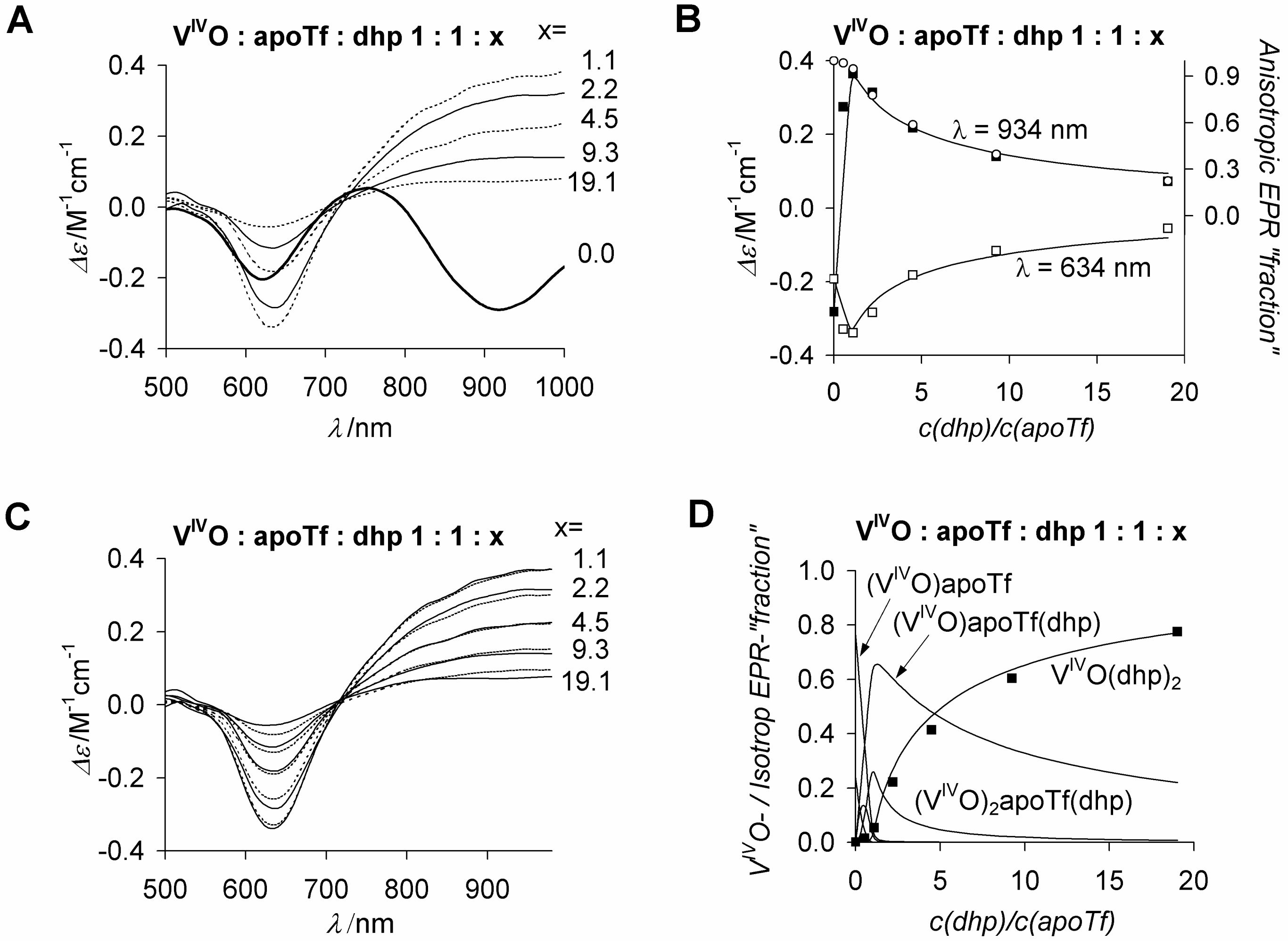

Figure S1

A Experimental CD spectra at different apoTf : dhp ratios (c(apoTf) = 0.77 mM, c($V^{IV}O$) = 0.77 mM)

B Experimental CD points and fitted curves at two selected wavelengths (□: λ = 634 nm, ■: λ = 934 nm, primary y axis). The "anisotropic fraction" of the EPR spectra (○, right y axis), calculated based on the ratio between the double integrated anisotropic part and the whole fitted spectrum, also depicted. The "anisotropic fraction" is the fraction of $V^{IV}O$ bound to apoTf. The experimental conditions are the same as in A.

C Several measured (solid) and calculated (dotted) CD spectra at the same condition

D Calculated speciation (based on stability constants in Table 1, c(apoTf) = 0.77 mM, c($V^{IV}O$) = 0.77 mM) during the titration of ($V^{IV}O$)apoTf with dhp (max. dilution ~20%). The isotropic "fraction" (■, same y axis) of the EPR spectra are also depicted.

(A-B-C-D: pH 7.4, c(HCO_3^-) = 25.0 mM, T = 25 °C).

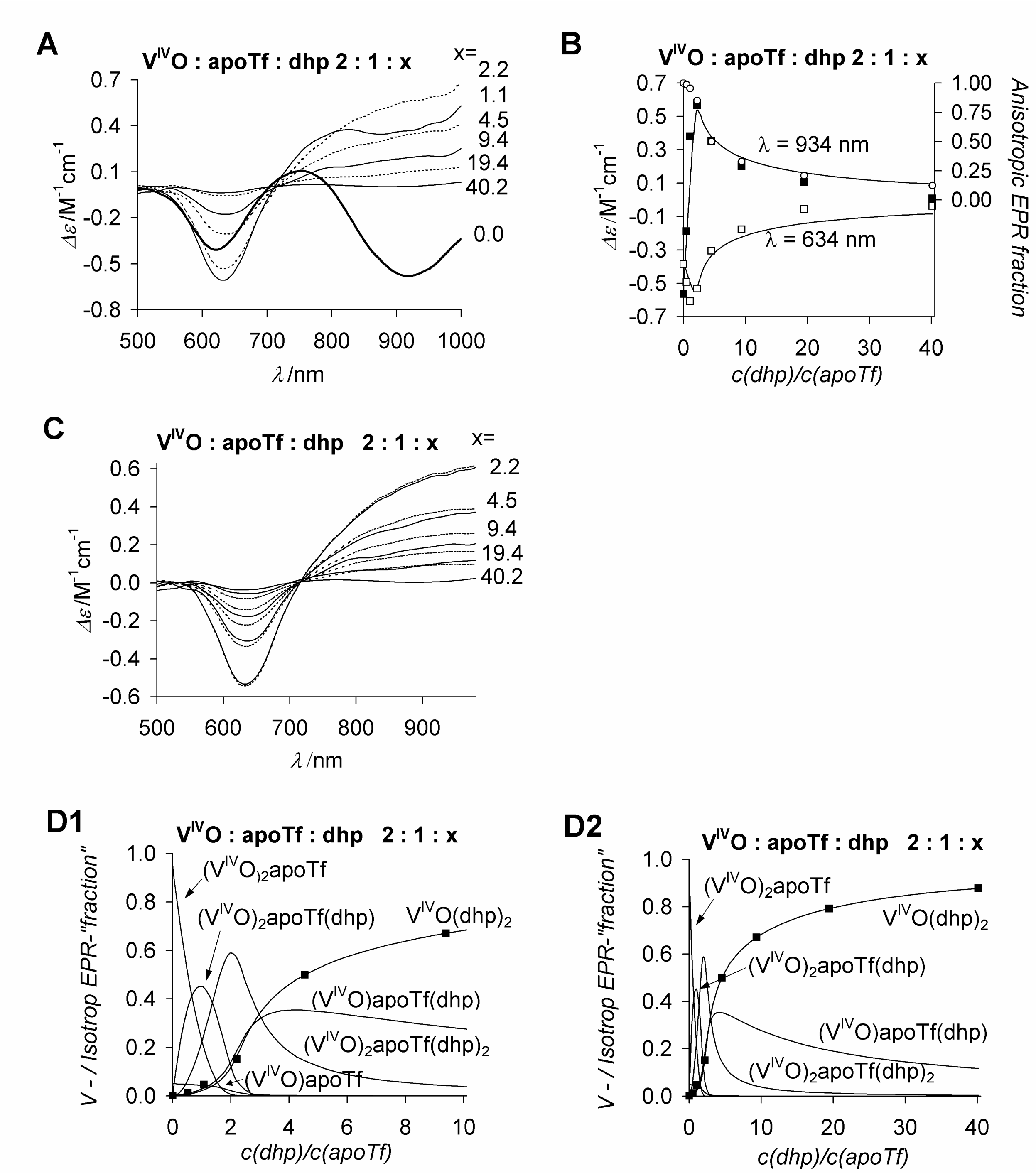

Figure S2

A Experimental CD spectra at different apoTf : dhp ratio (c(apoTf) = 0.51 mM, c($V^{IV}O$) = 0.98 mM)

B Experimental CD points and two fitted curve at two selected wavelengths (□ λ = 634 nm, ■ λ = 934 nm) and the anisotropic "fractions" (○, right y axis) of the decomposed EPR spectra.

C Several measured (bold) and calculated (thin) CD spectra at the same conditions

D1-D2 Calculated speciation curves as a function of the ratio of c(dhp)/c(apoTf), (based on the stability constants given in Table 1, c(apoTf) = 0.77 mM, c($V^{IV}O$) = 0.77 mM) during the titration of ($V^{IV}O$)apoTf with dhp (max. dilution ~20%). The isotropic "fraction" (■, depicted in the same y axis) of the EPR spectra are also given .

(A-B-C-D: pH 7.4, c(HCO_3^-) = 25.0 mM, T = 25 °C).

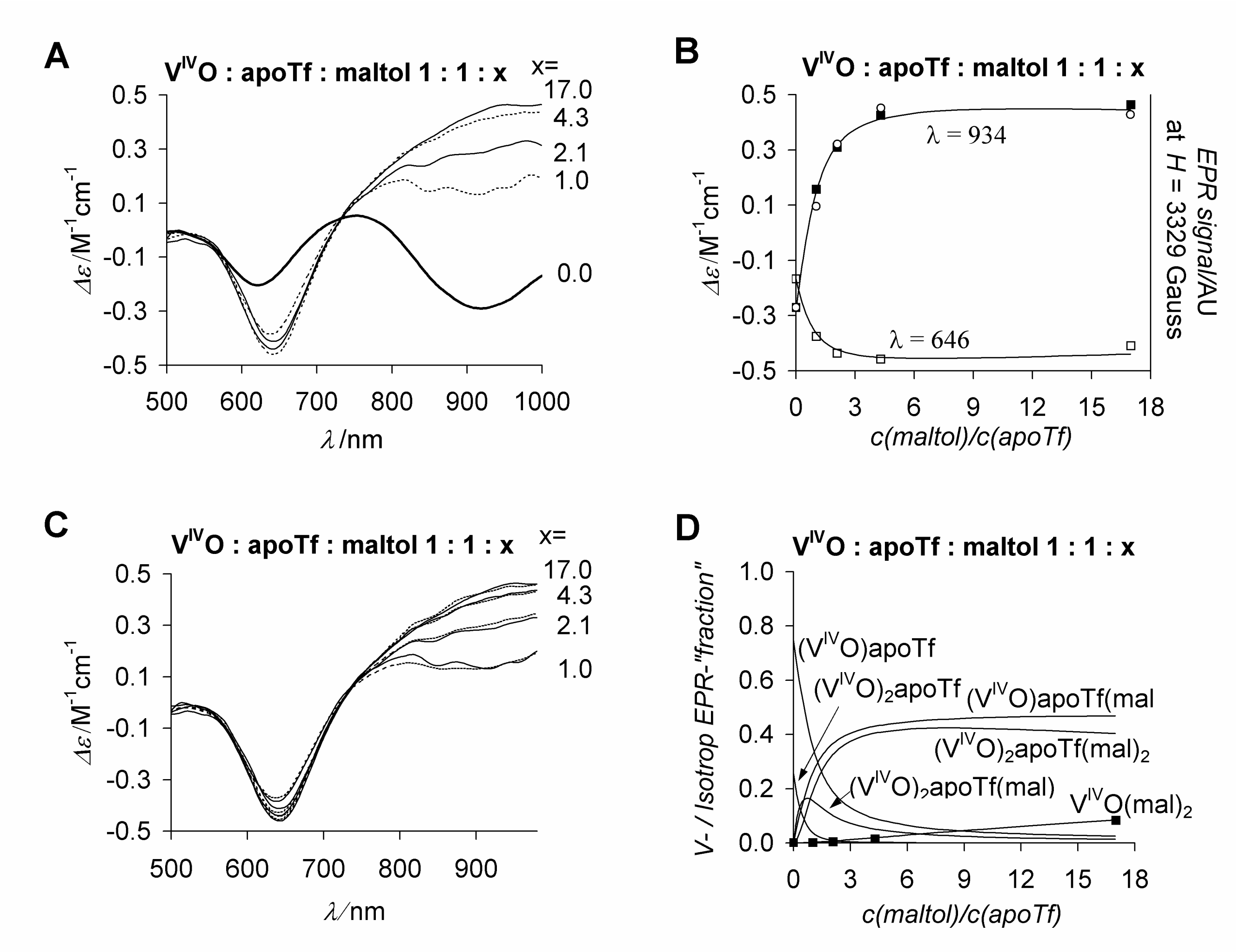

Figure S3

A Experimental CD spectra at different apoTf/maltol ratios (c(apoTf) = 0.89 mM, c($V^{IV}O$) = 0.89 mM)

B Experimental CD points and fitted curves at two selected wavelengths (□ λ = 646 nm, ■ λ = 934 nm) The intensity of the EPR signals (○, AU, right y axis) at *H* = 3329 Gauss (maximum of the $\perp_{7/2}$ transition of the ternary species) is also depicted. The experimental conditions are the same as in A.

C Several measured (solid lines) and calculated (dotted lines) CD spectra at the same conditions.

D Calculated speciation curves as a function of c(mal)/c(apoTf) ratio (based on the stability constants in Table 1, c(apoTf) = 0.89 mM, c($V^{IV}O$) = 0.89 mM during the titration of $(V^{IV}O)_2$apoTf with mal (max. dilution of ~20%). The isotropic “fraction” (■, depicted in the same y axis) of the EPR spectra representing the measured fraction of $V^{IV}O$ not bound to apoTf is also given.

(A-B-C-D: pH 7.4, c(HCO_3^-) = 25.0 mM, T = 25 °C).

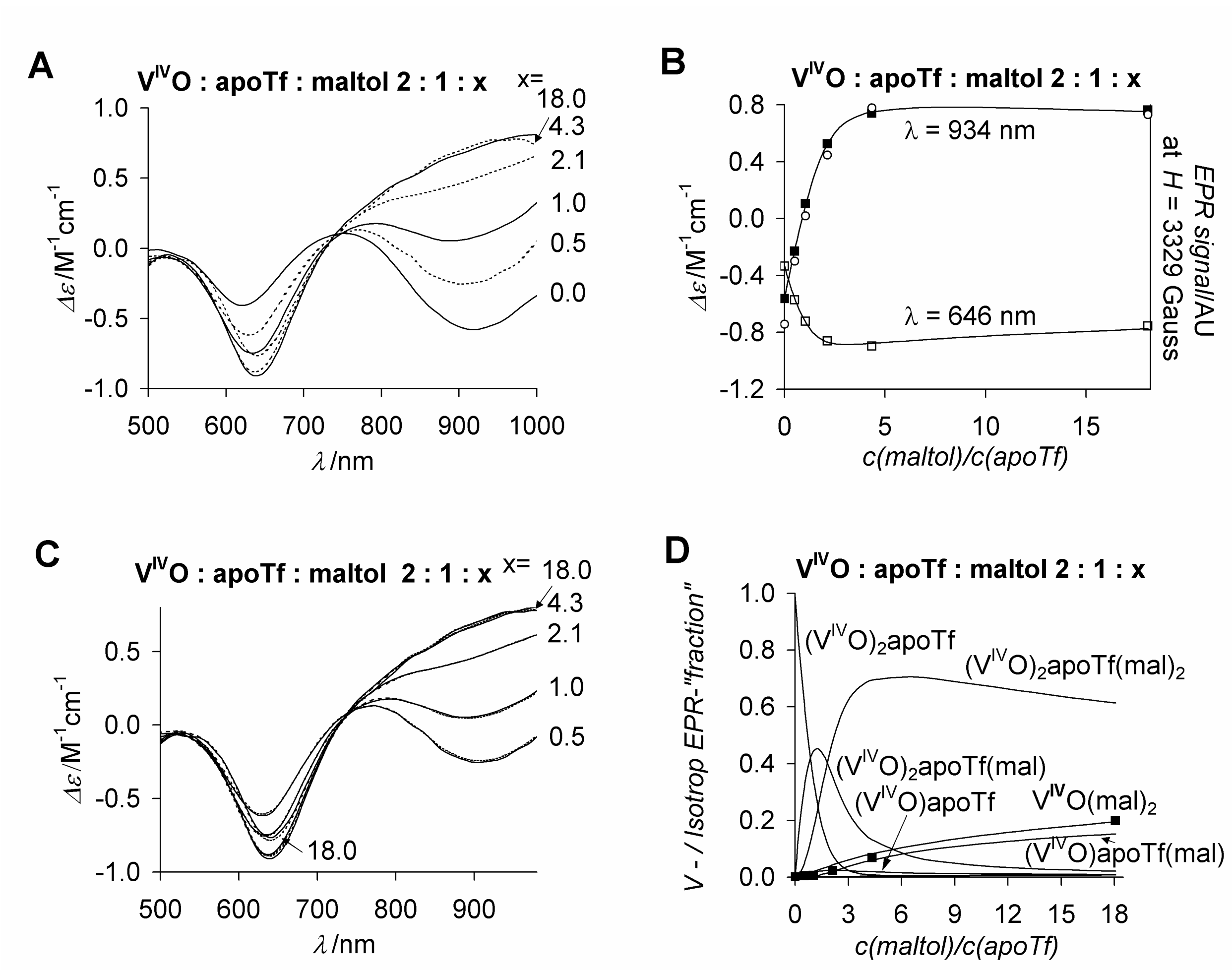

Figure S4

A Experimental CD spectra at different mal/apoTf ratios (c(apoTf) = 0.92 mM, $c(V^{IV}O) = 1.84$ mM)

B Experimental CD points and fitted curves at two selected wavelengths (□ λ = 646 nm, ■ λ = 934 nm) The EPR signal (○, AU, right y axis) at $H = 3329$ Gauss (maximum of the $\perp_{7/2}$ transition of the ternary species) are also depicted. The experimental conditions are the same as in A.

C Several measured (solid lines) and calculated (dotted lines) CD spectra at the same conditions.

D Calculated speciation (based on stability constants in Table 1, c(apoTf) = 0.92 mM, $c(V^{IV}O] = 1.84$ mM) during the titration of $(V^{IV}O)_2$apoTf with mal (max. dilution ~20%). The isotropic “fraction” (■, same y axis) of the EPR spectra, which practically represent the measured fraction of $V^{IV}O$ not bound to Tf is also depicted.

(A-B-C-D: pH 7.4, $c(HCO_3^-) = 25.0$ mM, T = 25 °C).

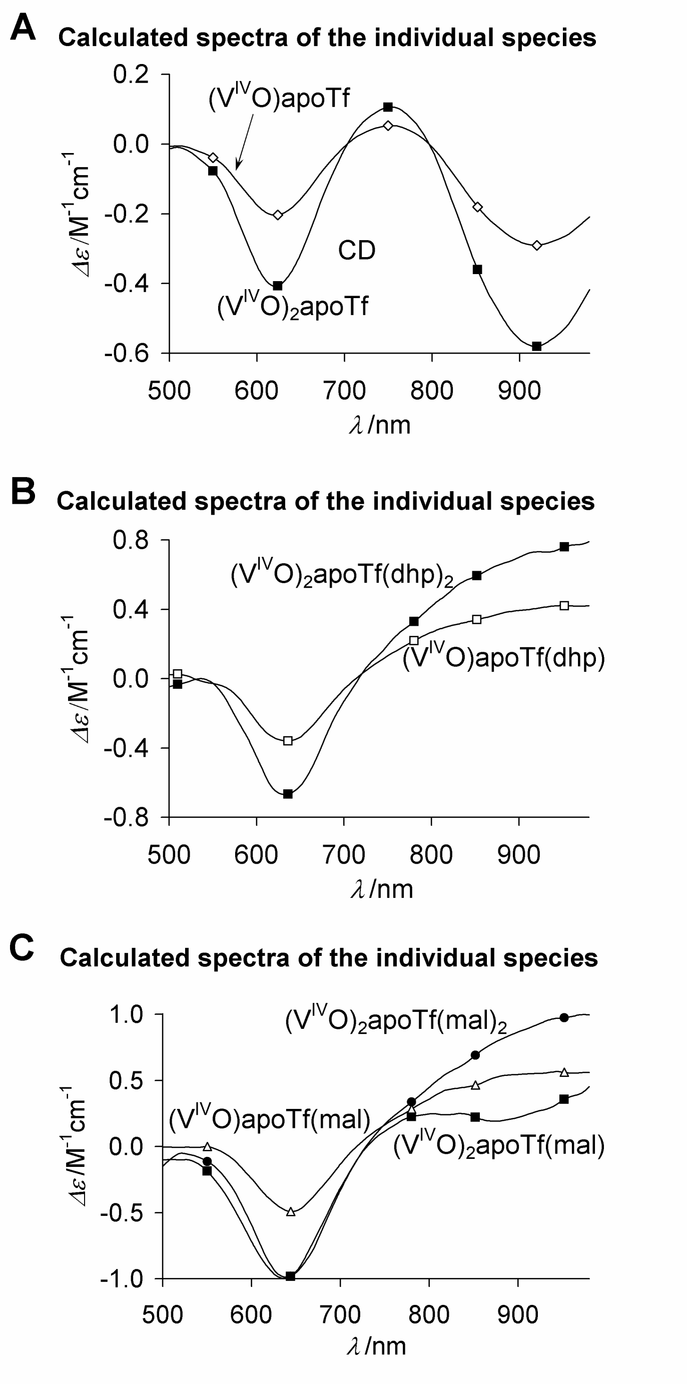

Figure S5

The calculated individual molar CD spectra of the binary and ternary complexes formed:

A

$(\mathrm{V^{IV}O})$apoTf (◇) and $(\mathrm{V^{IV}O})_2$apoTf (■)

B

$(\mathrm{V^{IV}O})$apoTf(dhp) (□) and

$(\mathrm{V^{IV}O})_2$apoTf(dhp)$_2$ (■)

C

$(\mathrm{V^{IV}O})$apoTf(mal) (△),

$(\mathrm{V^{IV}O})_2$apoTf(mal) (■), and

$(\mathrm{V^{IV}O})_2$apoTf(mal)$_2$ (●)

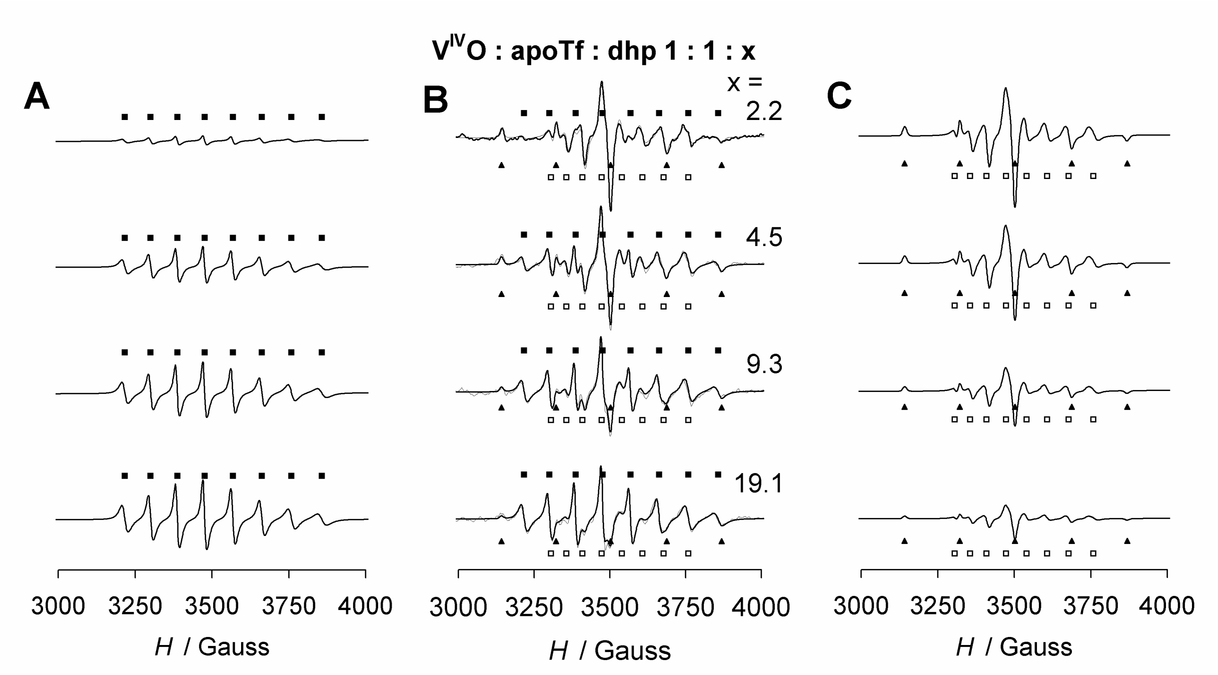

Figure S6 Simulation and "deconvolution" of some selected EPR spectra measured at different apoTf : dhp ratios (c(apoTf) = 0.77 mM, c($V^{IV}O$) = 0.77 mM, pH 7.4, c(HCO_3^-) = 25.0 mM, T = 25 °C), (■) isotropic, (□) ainisotropic, perpendicular and (▲) ainisotropic, parallel part of the spectra (The magnetic field range was reduced in the Figs. for a better clarity, the peaks $\|_{+7/2}$, $\|_{-5/2}$ and $\|_{-7/2}$ do not appear)

A Isotropic part of the selected simulated spectra

B Measured (thin) and simulated (bold) EPR spectra (Because of the good agreement of the measured and the simulated spectra they can be hardly distinguished.)

C Anisotropic part of the selected simulated spectra

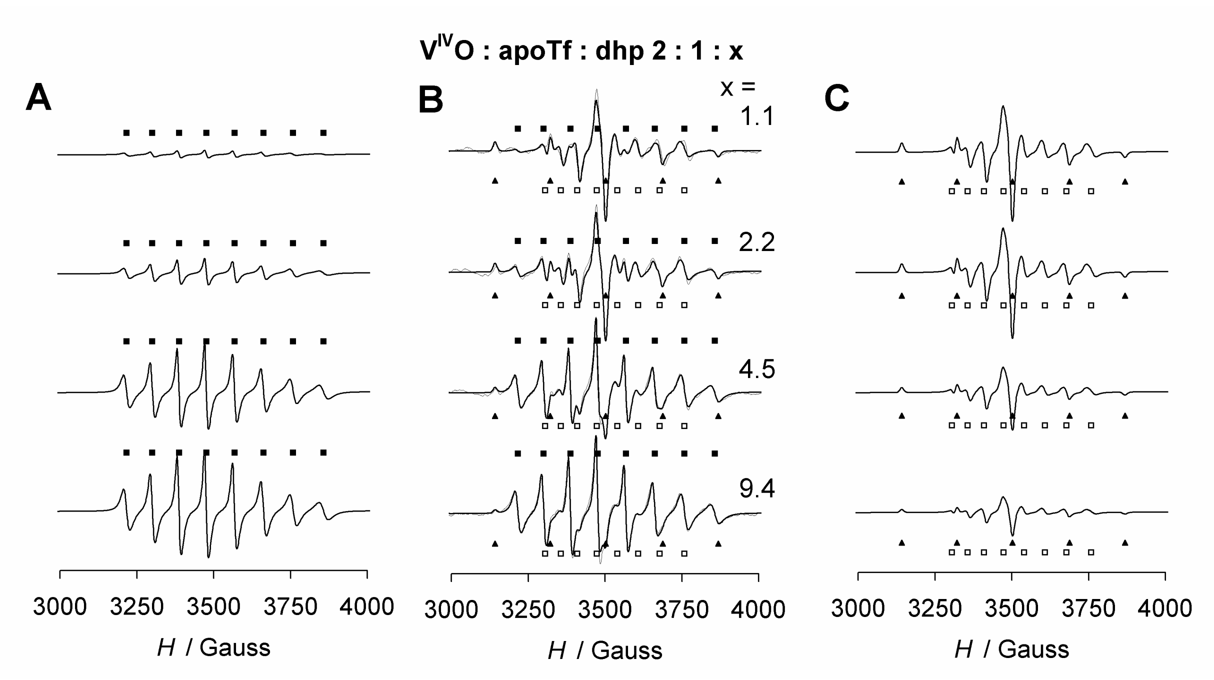

Figure S7 Simulation and "deconvolution" of some selected EPR spectra measured at different apoTf : dhp ratio (c(apoTf) = 0.51 mM, $c(V^{IV}O)$ = 0.98 mM, pH 7.4, $c(HCO_3^-)$ = 25.0 mM, T = 25 °C), (■) isotropic, (□) ainisotropic perpendicular and (▲) ainisotropic parallel (The magnetic field range of the figures was reduced in order for better clarity, the peaks $||_{+7/2}$, $||_{-5/2}$ and $||_{-7/2}$ do not appear)

A Isotropic part of the selected simulated spectra

B Measured (thin) and simulated (bold) EPR spectra (Because of the good agreement of the measured and the simulated spectra they can be hardly distinguished.)

C Anisotropic part of the selected simulated spectra

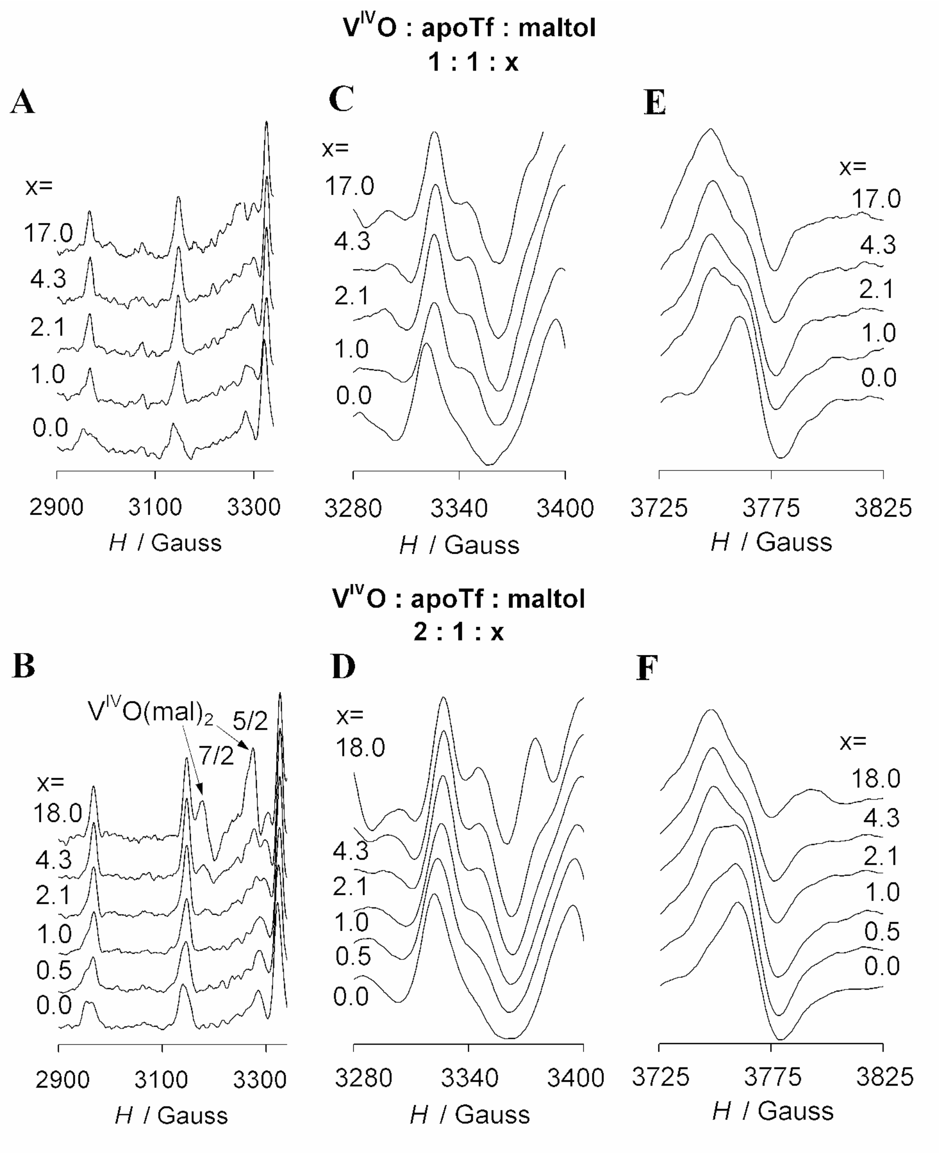

Figure S8

Amplifications of the EPR spectra measured at different $V^{IV}O$: apoTf : maltol ratio

(A, C, E : c(apoTf) = 0.89 mM, c($V^{IV}O$) = 0.89 mM; B, D, F: c(apoTf) = 0.92 mM, c($V^{IV}O$) = 1.84 mM; pH = 7.4, c(HCO_3^-) = 25.0 mM, T = 25 °C)

A-B The 2900-3320 Gauss range, mainly the $\parallel_{7/2}$, $\parallel_{5/2}$, $\perp_{7/2}$ and the $\parallel_{3/2}$ transition. At higher maltol content the isotropic 7/2 and 5/2 transitions can be observed.

C-D The 3280-3400 Gauss range (the $\parallel_{3/2}$ and the $\perp_{5/2}$ transition)

E-F The 3725-3825 Gauss range (the $\perp_{-7/2}$ transition)

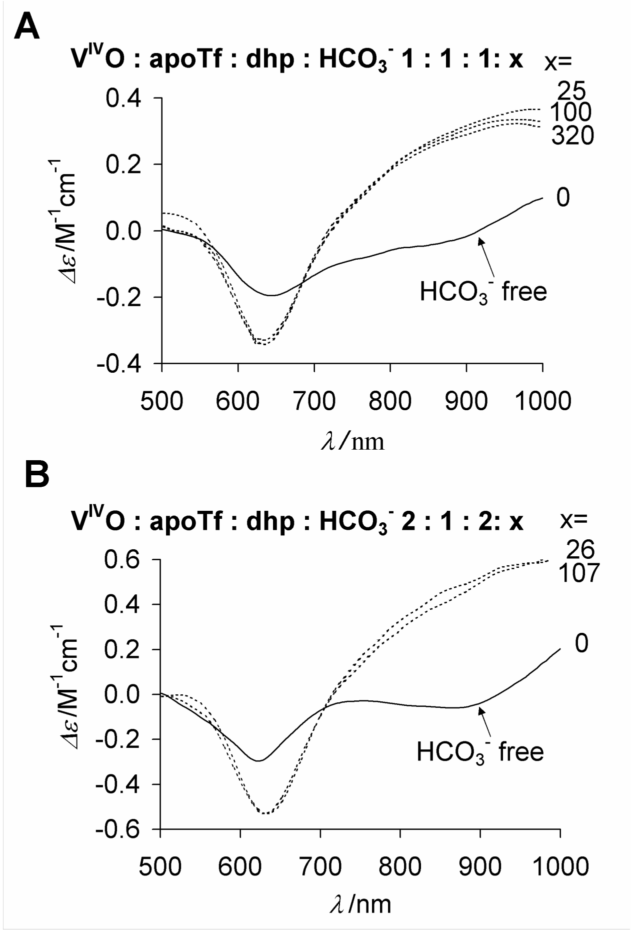

Figure S9

A CD spectra measured in the apoTf : $V^{IV}O$: dhp 1 : 1 : 1 system at different hydrogencarbonate concentration. (c(apoTf) = 0.93 mM, c($V^{IV}O$) = 0.93 mM, c(dhp) = 0.95 mM, pH 7.4, T = 25 °C)

B CD spectra measured in the apoTf : $V^{IV}O$: dhp 1 : 2 : 2 system at different hydrogencarbonate concentration. (c(apoTf) = 0.48 mM, c($V^{IV}O$) = 0.95 mM, c(dhp) = 0.94 mM, pH 7.4, T = 25 °C),

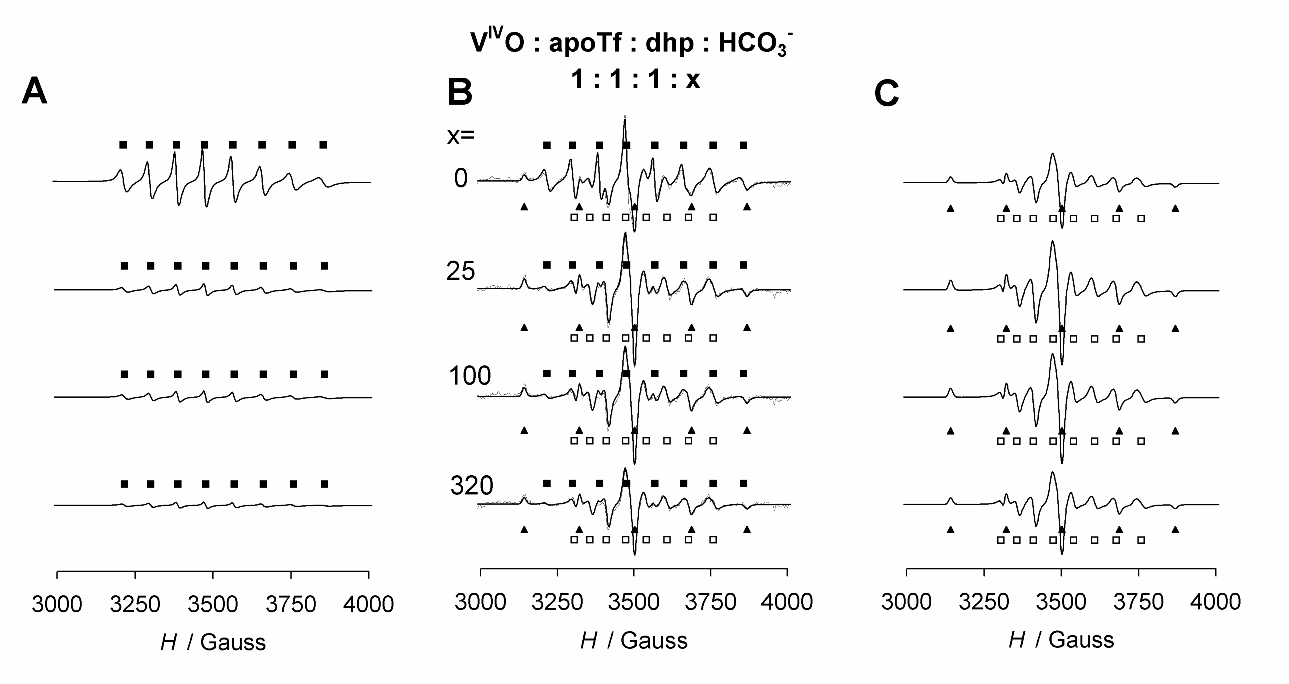

Figure S10 Simulation and "deconvolution" of EPR spectra measured in the $V^{IV}O$: apoTf : dhp 1 : 1 : 1 system at different carbonate concentration. (c(apoTf) = 0.93 mM, c($V^{IV}O$) = 0.93 mM, c(dhp) = 0.95 mM, pH 7.4, T = 25 °C), (■) isotropic, (□) ainisotropic perpendicular and (▲) ainisotropic parallel (The magnetic field range of the figures was reduced in order for better clarity, the peaks $||_{+7/2}$, $||_{-5/2}$ and $||_{-7/2}$ do not appear)

A Isotropic part of the selected simulated spectra

B Measured (thin) and simulated (bold) EPR spectra (Because of the good agreement of the measured and the simulated spectra they can be hardly distinguished.)

C Anisotropic part of the simulated spectra

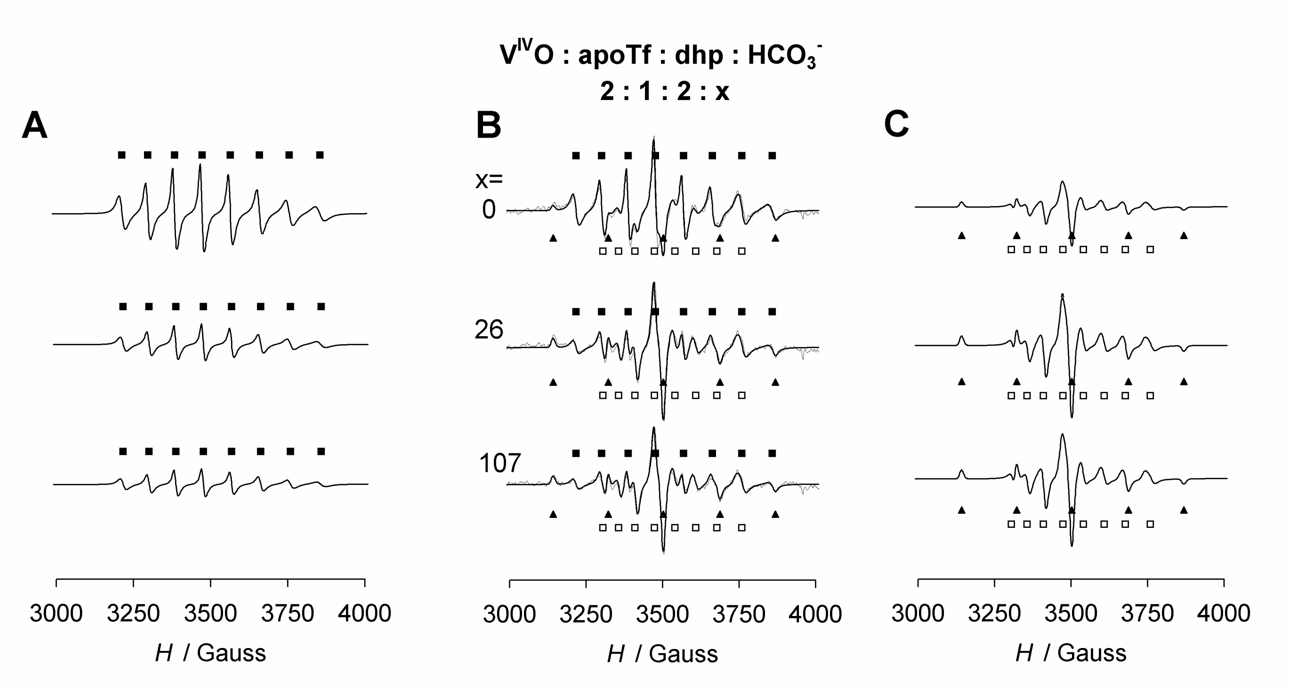

Figure S11 Simulation and "deconvolution" of EPR spectra measured in the $V^{IV}O$: apoTf : dhp 2: 1 : 2 system at different carbonate concentration. (c(apoTf) = 0.48 mM, c($V^{IV}O$) = 0.95 mM, c(dhp) = 0.94 mM, pH 7.4, T = 25 °C), (■) isotropic, (□) ainisotropic perpendicular and (▲) ainisotropic parallel (The magnetic field range of the figures was reduced in order for better clarity, the peaks $\|_{+7/2}$, $\|_{-5/2}$ and $\|_{-7/2}$ do not appear)

A Isotropic part of the selected simulated spectra

B Measured (thin) and simulated (bold) EPR spectra

C Anisotropic part of the simulated spectra

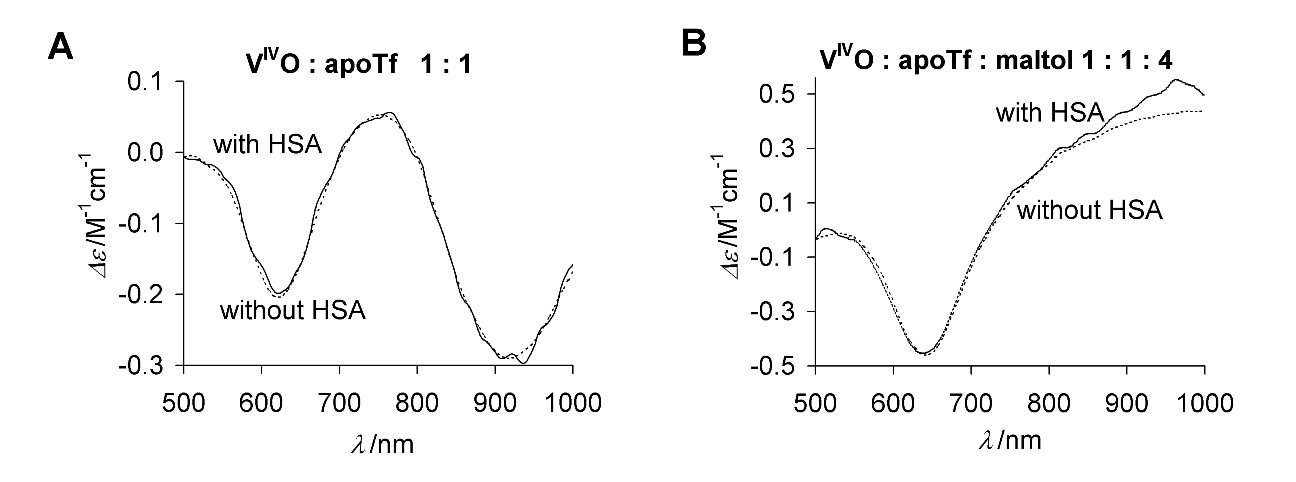

Figure S12 CD spectra of the $V^{IV}O$: apoTf : HSA 1 : 1 : 1 in the presence (**B**) and absence (**A**) of maltol; compared with the HSA free systems. The solid line spectra belong to HSA free the dotted line ones belong to the HSA containing samples. (c(apoTf) = 0.99 mM, c($V^{IV}O$) = 1.02 mM, c(HSA) = 1.00 mM, pH 7.4, c(HCO_3^-) = 25.0 mM, T = 25 °C) Order of addition: apoTf, $V^{IV}O$, HSA and maltol.